

AD-A157 363

THE ORIENTATION DISTRIBUTION OF NONSPHERICAL AEROSOL
PARTICLES WITHIN A CLOUD(U) HEBREW UNIV JERUSALEM
(ISRAEL) DEPT OF ATMOSPHERIC SCIENCES I GALLILY DEC 84
DAJA45-83-C-0004 F/G 20/4

1/1

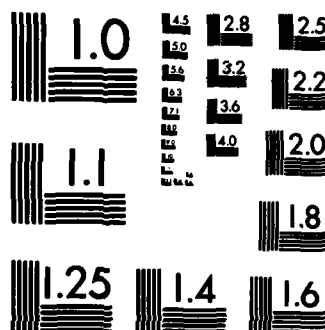
UNCLASSIFIED

NL

END

FIMIC

THE



MICROCOPY RESOLUTION TEST CHART
NATIONAL BUREAU OF STANDARDS-1963-A

AD-A157 363

4133-EN (7)

The Orientation Distribution of Nonspherical
Aerosol Particles within a Cloud

Second Technical Interim Report

by

Isaiah Gallily, Chief Investigator,
Department of Atmospheric Sciences,
The Hebrew University of Jerusalem,
Jerusalem, Israel

December, 1984

Contract DAJA 45-83-C-0004

United States Army Research, Development
and Standardization Group - UK,
London NW1, England

DTIC FILE COPY

DTIC
ELECTE
JUL 19 1985
S D
G

DISTRIBUTION STATEMENT A
Approved for public release;
Distribution Unlimited

Previous Publications: Krushkal, E.M. and Gallily, I., "On the Orientation Distribution Function of Nonspherical Aerosol Particles in a General Shear Flow. I. The Laminar Case", J. Colloid Interface Sci. 99, 141 (1984), and in the Proceedings of the 1983 CSL Conference on Obscuration and Aerosol Research, p. 19-58 (1984).

"The Orientation Distribution of Nonspherical Aerosol Particles in the Atmosphere; New Developments", in the Proceedings of the 1984 CRDC Conference on Obscuration and Aerosol Research (Draft for Presenters and CRDC Use), p. 57-68 (1984)

Accession For	
NTIS GRA&I	
DTIC TAB	
Unannounced	
Justification	
By	
Distribution	
Availability Codes	
Dist	Availability
A1	

The models

Having performed a study on the orientation density function (o.d.f.) of small spheroidal aerosol particles in a general field of an arbitrary strength, (1,2) it became possible to treat the orientation problem in a turbulent medium. To this end, two interconnected physical models were applied. In the first, "The Realizations Model," it was assumed that the turbulent particle field constituted an ensemble of an infinite number of realizations, j , each one of which is characterized by one set of the o.d.f., $F^{(j)}(x,t)$, values. The latter was taken in that model to essentially coincide with the previously found solution of the Fokker-Planck equation (1,2) in the field of the realization. *→ next page*

$$\partial F^{(j)} / \partial t - \nabla \cdot [\omega (W_{ik}^{(j)}, R) - \alpha_e^{-1(j)} \nabla F] = 0 \quad (1)$$

where ω is the rotational velocity of the particles and $\alpha_e^{(j)}$ is their rotational Peclet number defined by W_0 / D_e , W_0 being a typical component of the (fluid) gradient tensor, D_e an effective rotational diffusion coefficient and R the particle aspect ratio; W_{ik} is a gradient component $\partial u_i / \partial x_k$ (u_i - a component of the fluid velocity). The use of the solution is based on the estimate that, even for the highest (Kolmogoroff) frequency component of u_i , the rotational Reynolds number for the studied particles is small enough to render their motion (quasi) stationary.

In the second, "The Micro-turbulence Model," a relation between the so-called turbulent rotational diffusion coefficient r_{D_t} of the particles and the physical characteristics of the fluid field was supplied. This coefficient and the Brownian rotational diffusion one, r_{D_B} , compose the effective diffusion coefficient,

$$r_{D_e} = r_{D_t} + r_{D_B} . \quad (2)$$

Expressing the stochastic quantities of the system as $F = \bar{F} + F'$, $\omega_i = \bar{\omega}_i + \omega'_i$, $w_{ik} = \bar{w}_{ik} + w'_{ik}$ and $u_i = \bar{u}_i + u'_i$, it could be shown that the realizations' average of F , $\bar{F}(w'_{ik}, r_{D_B}, R)$, for a space-time point is actually $F(\bar{w}_{ik}, r_{D_e}, R)$ for that point and that

$$\omega' F' = - r_{D_t} \nabla F . \quad (3)$$

The particles considered were taken to be much smaller than the Kolmogoroff scale; so, the turbulent rotational diffusion coefficient itself, r_{D_t} , was assumed in the second model to depend on the randomizing action of the turbulent pressure fluctuations at the particles' surface which arise from the (Kolmogoroff) micro-turbulence.

From dimensional analysis it was obtained that

$$r_{D_t} = (\epsilon / \eta)^{1/2} \quad (4)$$

where ϵ , the turbulent dissipation energy, is given for an homogeneous steady field by (3)

$$\epsilon = \eta \sum_{i,k} \overline{w'_{ik}{}^2} . \quad (5)$$

Applications

As the turbulent gradient tensor W'_{ik} is not completely known in many fluid systems, it was necessary in the present study either to supplement the missing data by the results of numerical simulations or (reasonable) guesses or both. In cases of interest, there was conducted a parametric investigation in which the effect of structure changes in the gradient tensor on the o.d.f. was tested.

The numerical simulations of the turbulent field were carried out according to the method of Wang and Frost (4) where $u'_i = u'_i(t)$ is found. In this method, however, only the three components W'_{i1} ($i = 1, 2, 3$) could be acquired due to the applicability of the relationship known as the Taylor hypothesis, viz.

$$\partial u'_i / \partial t = -\bar{u}_i \partial u'_i / \partial x, \quad (6)$$

to those components alone.

The rest of the gradient components were extracted either from the experimental findings of Klebanoff (5) for the studied situations of a turbulent flow over a flat surface as in the atmospheric boundary layer or from those of Wignansky and Fiedler (6) for the studied situation of a free round turbulent jet, or from parametric checks as mentioned above. The experimentally acquired gradient components are given in the form of $\Delta W'_{ik} = (\overline{W'^2_{ik}})^{1/2}$ and so were taken the rest of the components. The (turbulent) fluid was assumed to be incompressible, viz. $W'_{ii} = 0$, and it was set that

$$\Delta W'_{22} = \Delta W'_{33} = -\frac{1}{2} \Delta W'_{11} \quad (7)$$

or with reversed signs.

Obviously, since in addition to the average value of F , \bar{F} , or its maximal value F_m , some measure of the spread of the o.d.f. values is desired, a procedure was adopted in which this (F) function was calculated for the following three realization fields:

$$(1) \quad W^{(i)}_{ik} = \bar{W}_{ik}, \quad (8a)$$

$$(2) \quad w_{ik} = \bar{w}_{ik} - \Delta w_{ik}^i \quad (8b)$$

and

$$(3) \quad w_{ik} = \bar{w}_{ik} + \Delta w_{ik}^i \quad (8c)$$

Finally, to account for any uncertainties in the turbulent field data, the (determining) effective Peclet number was parameterized by a numerical factor to be

$$\alpha_e \quad \alpha_o = W_o / D_e \quad (9)$$

where W_o , w_o , w_o' , $w_o' [= (\Delta w_{ik}^i)_o]$ being a typical turbulent component.

Results

Two physical situations were studied:

1. The near-ground atmospheric boundary layer, in which only

$$u_1(z) = (u^*/k_o) \ln(1 + z/z_o) \quad (10)$$

and

$$\bar{w}_{13} = \partial \bar{u}_1 / \partial z = u^* / k_o(z - z_o) \quad (11)$$

essentially exist, z being the elevation above ground, \bar{u}_1 the mean horizontal velocity, u^* the friction velocity, k_o von Karman Constant and z_o the roughness height.

2. The turbulent round free jet, for which the Schlichting's solution for the average velocity components (7) was used. In this solution, the (molecular) kinematic viscosity ν is replaced by a virtual (turbulent) kinematic viscosity ϵ_0 given in the equation

$$\epsilon_0 = 0.161 J'^{1/2} \quad (12)$$

where $J' (=J/\nu) = 1.59 \cdot b_{1/2} \bar{u}_0$, J' is the kinematic momentum of the jet, $b_{1/2}$ is its half-width and u_0 is the average fluid velocity along its axis ($b_{1/2} = cx_1$ in which c is 0.63 to 0.79, as experimentally found).

In the boundary layer situation, both the case of a "weak turbulence", where $w'_0 \approx \bar{w}_0$, and a "strong turbulence", where $w'_0 \gg \bar{w}_0$, were investigated.

For the first case, numerical simulations were employed while for the second one Klebanoff's experimental data (5) supplemented by simulations was applied. Also, in the latter case, the version

$$\overline{w'_{32}}^2 = \overline{w'_{23}}^2 = \overline{w'_{13}}^2 \quad (13a)$$

or

$$\overline{w'_{32}}^2 = \overline{w'_{23}}^2 = \overline{w'_{11}}^2 \quad (13b)$$

was taken. The calculations in both cases were carried out with $\nu = 0.15 \text{ cm}^2/\text{sec.}$, δ (thickness of the atmospheric boundary layer) = 10^3 m , $z_0 = 0.1 \text{ m}$, $k_0 = 0.4$, $r_{DB} = 1 \text{ sec}^{-1}$, and ϵ deduced from Eq. (5). The calculation time for \bar{F} was greater than the relaxation time of the particles, and $\Delta\theta = \Delta\phi = \pi/12$ or $\pi/24$.

In the turbulent jet situation, the ratio between the various values of was obtained (6) through

$$c_2 \overline{W'_{ik}^2} = \overline{W'^2} \quad (i, k = 1, 2, 3) \quad (14)$$

where $c_2 = 1 + \exp(-200r^2)$, r being the radial distance within the jet.

For both situations, the absolute values of $\Delta W'_{ik}$ were deduced by normalization according to Eq. (5). Values of \overline{F} , and F_m , together with the deviations of F for fields (2) & (3) (above), were calculated as a function of height above ground (and hence ϵ) in the boundary layer situation, the aspect ratio of the particles, R ($R > 1$ for fibers and $R < 1$ for platelets), and the parameterization factor α_0 . However, only the following typical figures are presented here:

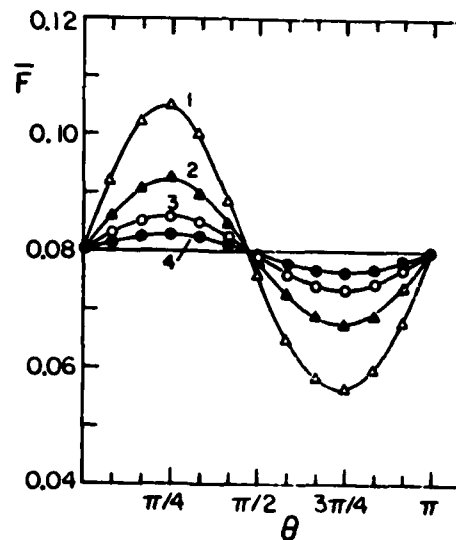


Figure 1. The average o.d.f., \overline{F} , vs. θ for the atmospheric boundary layer, "weak turbulence", with:

$z = 2.5$ to $20m$ (1) $2.5m$, (2) $5m$, (3) $10m$, (4) $20m$,

$R = 10$, $\phi_m = \pi/2$,

$\alpha_e = 1$, $\overline{W}_{13}(=\overline{W}_0)$ according to Eq. (11), $W'_0 = \Delta W'_{13}$.

Solid lines are simulation results (254 realizations, usually); points are values calculated from the \overline{W}_{ik} field.

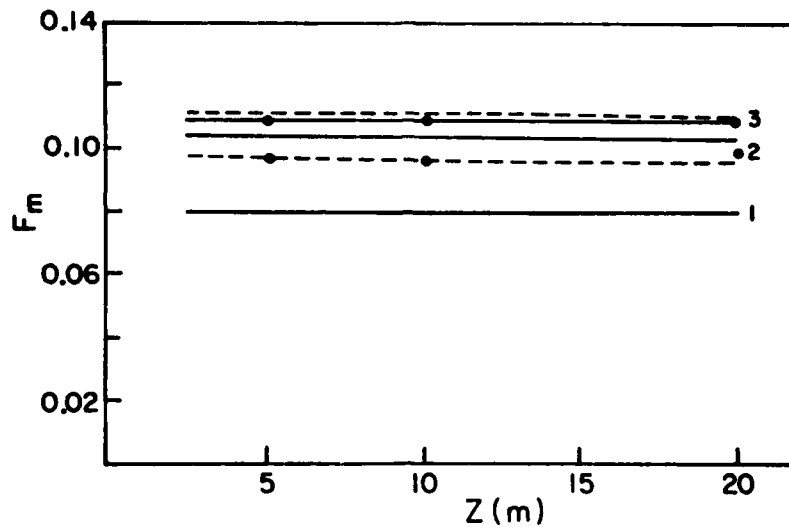


Figure 2. The maximal o.d.f., F_m , vs. height for the atmospheric boundary layer, "strong turbulence". $R = 50$; ϵ decreases with height according to Ball (8).

(1) $W_{i,n}^{(1)}$, (2) $W_{i,n}^{(2)}$, (3) $W_{i,n}^{(3)}$; dashed lines are cases where terms of Eq. (7) are taken with opposite signs; points relate to combination of Eq. (13b).

(Line 1 essentially coincides with the random distribution one)

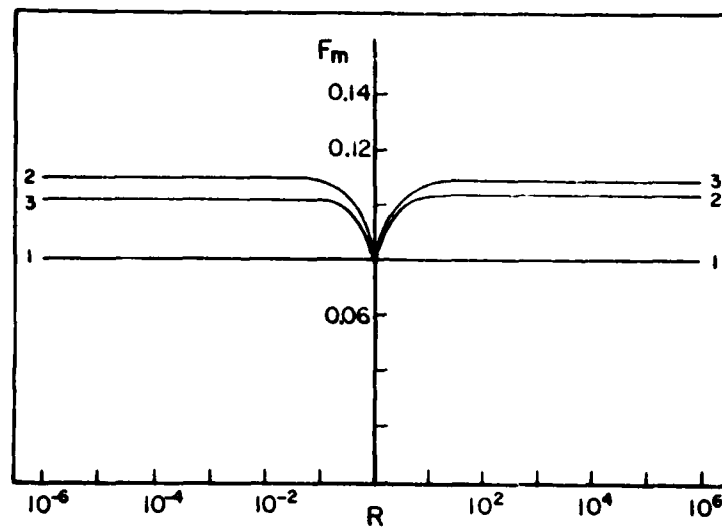


Figure 3. The maximal o.d.f., F_m , vs. particle aspect ratio R for the atmospheric boundary layer, "strong turbulence".

$$z = 5m, \epsilon = 230 \text{ cm}^2/\text{sec}^{-3}$$

$$(1) W_{ik}^{(1)}, (2) W_{ik}^{(2)}, (3) W_{ik}^{(3)}$$

(Line 1 essentially coincides with the random distribution one)

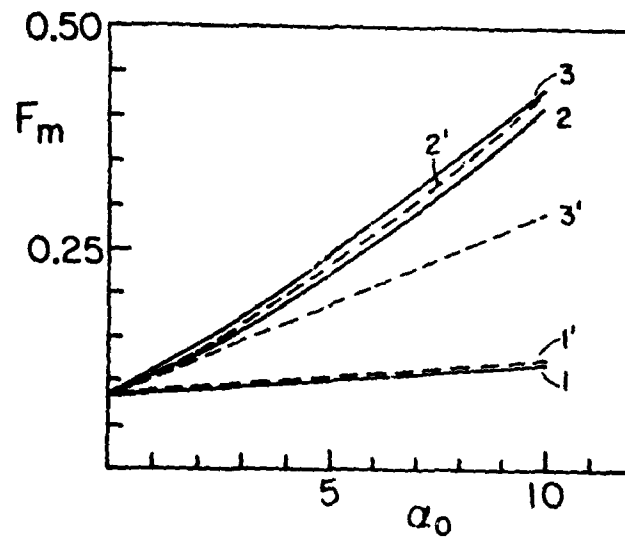


Figure 4. The maximal o.d.f. F_m vs. the parameter α_0 for the atmospheric boundary layer; "strong turbulence".

$R = 50$ ——— ; $R = -.02$ - - - - ; $z = 2.5m$; $\epsilon = 5 \text{ cm}^2/\text{sec}^3$.

(1) $w_{ik}^{(1)}$, (2) $w_{ik}^{(2)}$, (3) $w_{ik}^{(3)}$

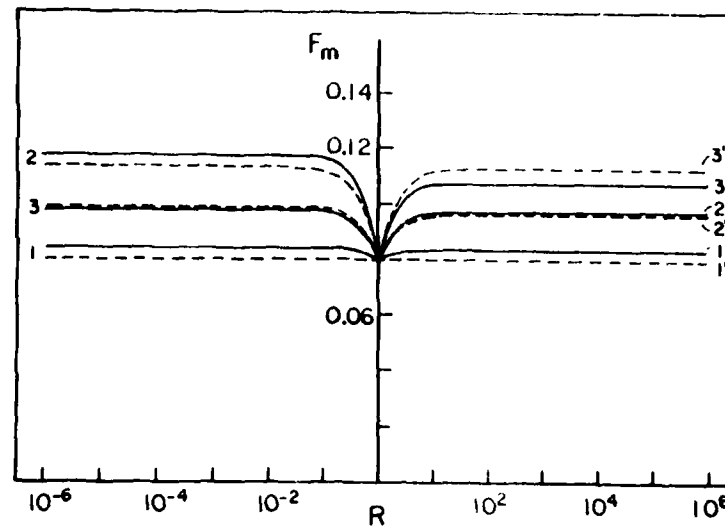


Figure 5. The maximal o.d.f., F_m , vs. particle aspect ratio R for a free turbulent jet.

Location: $x_1 = 2$, $x_2 = x_3 = 0.05$ (see ref. 1),

$$\bar{u}_0 = 5 \text{ sec}^{-1}, \quad \epsilon = 250 \text{ cm}^2/\text{sec}^3$$

(1), (1'): $W_{ik}^{(1)}$; (2), (2'): $W_{ik}^{(2)}$; (3), (3'): $W_{ik}^{(3)}$; for (1'), (2'), (3') terms of Eq. (7) are taken with opposite signs.

(Line 1 essentially coincides with the random distribution one)

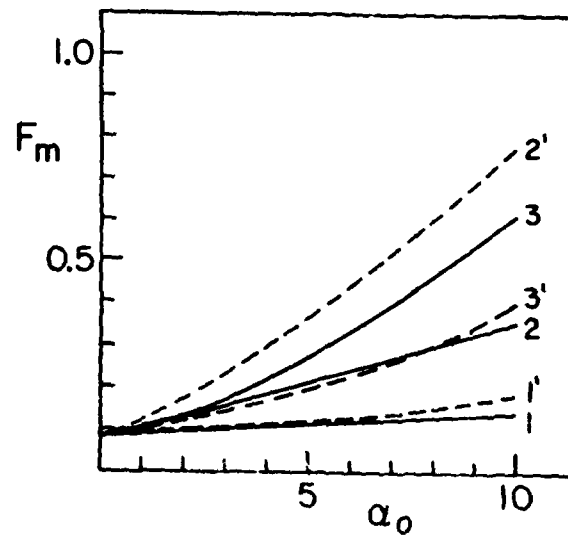


Figure 6. The maximal o.d.f., F_m vs. the parameter α_0 for a free turbulent jet.

$$\bar{W}_0 = 5 \text{ sec}^{-1}, x_1=2, x_2=x_3=0.05 \text{ (see ref. 1)}$$

$$\epsilon = 125 \text{ cm}^2/\text{sec}^3, R = 50 \text{ —————}, R = 0.02 \text{ - - - - -}$$

Conclusions

Atmosphere boundary layer (up to 20 m height):

1. The average o.d.f. in a weak turbulent field shows structured (preferred) orientation.
2. The maximal (and average) o.d.f. in a strong, commonly occurring, turbulent field of the average realization $W_{ik}^{(1)}$ essentially coincide with the random distribution while the spread of the values of the function between fields $W_{ik}^{(2)}$ and $W_{ik}^{(3)}$ is quite significant. This spread of values may have practical connotations.
3. The values of F_m and its deviations increase with the parameter as expected.

Free turbulent jet:

Conclusions 2 and 3 of the former situation apply here too.

References

1. E.M. Krushkal and Isaiah Gallily, J. Colloid Interface Sci. 99, 141 (1984).
2. Isaiah Gallily and R.M. Krushkal, Proceedings of the 1983 CSL Conference on Obscuration and Aerosol Research, p. 49-58 (1984).
3. Hinze, J.O., "Turbulence," McGraw-Hill, Inc. (1975).
4. Wang, S.T., and Frost, W., NASA CR 3309 (1980).
5. Klebanoff, P.A., NACA TN 3178 (1954).
6. Wignansky, I., and Fiedler, H., J. Fluid Mech. 38, 577 (1969).
7. Schlichting, H., "Boundary Layer Theory" McGraw-Hill Inc. (1968) pp. 220, 699.
8. Ball, F.K., J. Meteorol., 18, 553 (1961).

END

FILMED

9-85

DTIC